High-speed broadband FTIR system using MEMS

N. Pelin Ayerden,[1,2] Ugur Aygun,[1] Sven T. S. Holmstrom,[1] Selim Olcer,[1] Basarbatu Can,[1] Jean-Louis Stehle,[3] and Hakan Urey[1,*]

[1]Department of Electrical Engineering, Koc University, Istanbul 34450, Turkey

[2]Microelectronics Department, Delft University of Technology, Delft 2628 CD, The Netherlands

[3]Semilab, Budapest H-1117, Hungary

*Corresponding author: hurey@ku.edu.tr

Received 31 July 2014; revised 23 September 2014; accepted 23 September 2014; posted 23 September 2014 (Doc. ID 217555); published 23 October 2014

Current Fourier transform infrared spectroscopy (FTIR) systems have very good spectral resolution, but are bulky, sensitive to vibrations, and slow. We developed a new FTIR system using a microelectromechanical system (MEMS)-based lamellar grating interferometer that is fast, compact, and achromatic (i.e., does not require a beam splitter). The MEMS device has >10 mm^2 active surface area, up to ±325 μm mechanical displacement, and a 343 Hz resonant operation frequency. The system uses a 5 MHz bandwidth custom infrared (IR) detector and a small emission area custom blackbody source to achieve fast interferogram acquisition and compact form factor. Effects of lamellar grating period, detector size, laser reference, apodization, and averaging of data on the spectral resolution are discussed. The measurement time ranges from 1.5 to 100 ms depending on the averaging time. In the target range of 2.5–16 μm (625–4000 cm^{-1}) a spectral resolution of 15–20 cm^{-1} is demonstrated. The measurements are shown to be stable over a long time. © 2014 Optical Society of America

OCIS codes: (120.6200) Spectrometers and spectroscopic instrumentation; (300.6300) Spectroscopy, Fourier transforms; (050.0050) Diffraction and gratings; (230.4685) Optical microelectromechanical devices.

http://dx.doi.org/10.1364/AO.53.007267

1. Introduction

Fourier transform infrared spectroscopy (FTIR) has been the gold standard in infrared (IR) spectroscopy since the 1970s [1–3]. FTIR instruments have, however, traditionally been bulky, sensitive to vibrations, and needed at least several seconds per measurement. There is a long-term trend toward ever smaller systems and with the large developments in microelectromechanical systems (MEMS) over the last two decades it is now possible to realize truly miniaturized FTIR instruments that are cheaper, faster, and more convenient to use [4–6]. Miniaturized FTIR spectrometry is of interest in a very wide array of applications, including food monitoring, gas detection, bomb detection, the mining industry, space missions, and quality and process control.

FTIR is usually implemented with a moving mirror in the Michelson configuration [7] and successful MEMS implementations of this type have been reported [8,9]. An alternative approach is the lamellar grating interferometer (LGI), where the wavefront is split by having one half reflected from the moving binary grating fingers and the other half from the static grating fingers [10]. The LGI configuration has several advantages that make it especially suited for easy-to-handle, mobile instruments. LGI enables a more compact optical setup since the dynamic grating eliminates the reference mirror, beam splitter, and dispersion compensation plates. The simpler assembly and the combination of dynamic and static mirrors in one single component make for greater robustness. On the optical side it is possible to implement the LGI-based system with only

1559-128X/14/317267-06$15.00/0

reflective components, rendering it achromatic and enabling simultaneous spectrum measurements in multiple wave bands by changing the detector only, which is a distinct advantage over traditional FTIRs. Additionally, since the moving element is a grating rather than a solid mirror, LGIs lend themselves to implementations without vacuum packaging. All measurements in this paper are performed at ambient pressure.

The theoretical background of the LGI spectrometer is described elsewhere [11–13]. The mechanical design, fabrication, and characterization of the MEMS interferometer used here are given in [14]. With a clear aperture of 10 mm^2 and an operational deflection up to ±325 μm the present device has the largest clear aperture as well as the largest displacement of any non-Michelson MEMS spectrometer device. Spectrums measured with and without laser reference are presented and signal processing choices are discussed in this paper. The device is operated at resonance around 343 Hz, with two full spectrums obtained per cycle. One spectrum is hence measured in 1.5 ms. This makes room for measurement times far below 1 s even with optimal averaging. Resonant operation improves the measurement time drastically compared to its counterparts. A MEMS Michelson interferometer with a thermally actuated gear and crank system was reported to have a full cycle of 600 μm displacement in just over 1 s [15]. An electrostatically actuated LGI was presented with 145 μm optical path difference (OPD) measured step by step in 5 min [13]. Apart from our device, a MEMS Michelson interferometer that operates in the resonant mode at 500 Hz is reported to have a measurement time of 1 ms [8].

In Section 2 we develop a bench-top setup for an LGI-based FTIR spectrometer, using the above-mentioned MEMS device, for measurement in the 2.5–16 μm (625–4000 cm^{-1}) range. In Section 3 we analyze and compare spectrum measurements taken in different conditions. In Section 4 the paper is concluded.

2. Optical Design and Optimization

The layout of the FTIR spectrometer setup is shown in Fig. 1(a). Infrared radiation from the source is collimated by a 90° off-axis parabolic mirror and then reflected off the lamellar grating. After passing through the sample, the beam is focused onto the IR detector by the focusing lens and aligned so that only the zeroth diffraction order reaches the sensor. The IR source (developed by Bruker Optics, Germany) is a blackbody radiator operating at 1070 K with an emission diameter of 0.5 mm. The IR detector (developed by VIGO Systems, Poland) is a thermoelectrically cooled HgCdTe detector with an integrated 12.85 mm focal length focusing lens. The detector and source are both designed specifically for this project and the target range of 2.5–16 μm (625–4000 cm^{-1}). To accurately track the device deflection, a reference laser of He–Ne type (632.8 nm) is diffracted off the grating. The reference

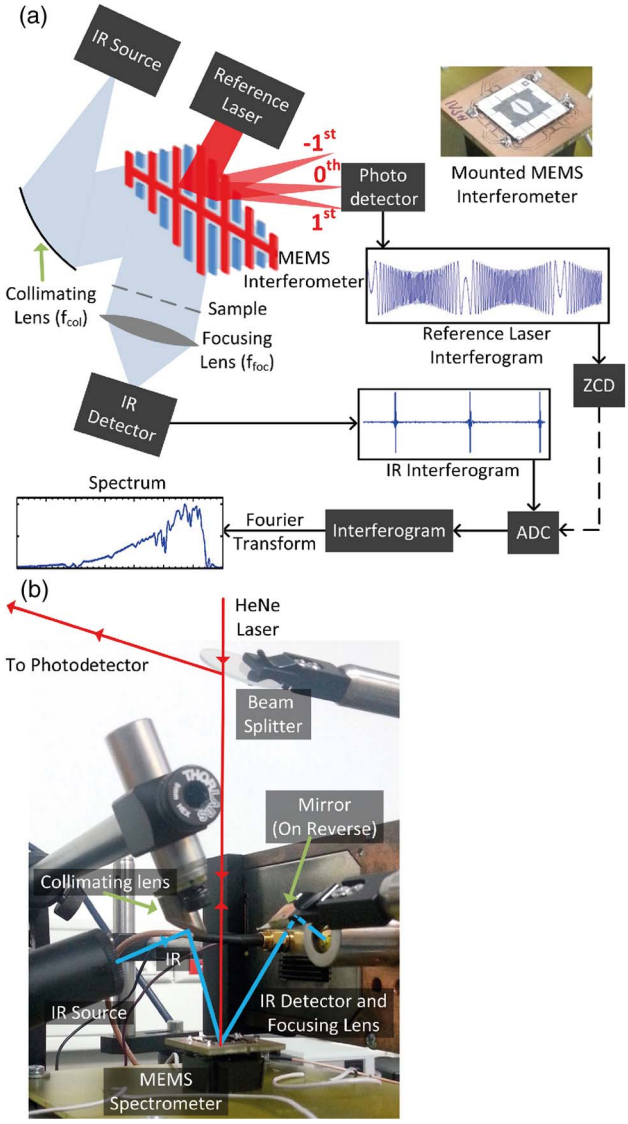

Fig. 1. (a) Schematic of the spectrometer system setup. ZCD, zero-crossing detector; ADC, analog-to-digital converter. (b) Our actual spectrometer implementation. Note that in the actual setup both IR and laser reference are reflected off the front side of the device.

data is acquired by capturing the zeroth order with a photodetector.

Since the resonant device motion is sinusoidal, the IR interferogram is resampled at the zero crossings of the laser interferogram to obtain a spatially equidistant IR interferogram. The Fourier transform of this resampled data will then give the spectrum. Each spectral measurement consists of two separate steps: a reference measurement without the sample is followed by a measurement with the sample placed in the optical path. After data sampling and Fourier transform, percent transmittance and absorbance spectra are calculated in MATLAB. In order to increase the SNR, averaging and apodization may be applied to the interferogram.

The general reasoning and method behind the optical design consideration are treated in [12].

The MEMS interferometers are fabricated with a four-mask SOI bulk micromachining process. Each device has an Al top reflector, 11 mm × 11 mm die area, 130 μm grating pitch, and a 10 mm^2 clear aperture. The grating consists of alternating static and movable mirrors, arranged in a diamond pattern to increase the efficiency for a circular beam. For the measurements in this paper deflections up to ±325 μm are used; all achieved with acoustic actuation at 343 Hz.

The spectral resolution of LGI-based FTIR spectrometers are restricted by four main limitations: OPD created by the interferometer, the Talbot effect, diffraction order mixing, and divergence of the source. The OPD is twice the zero-to-peak deflection. The highest possible spectral resolution is 1/OPD, which is around 15 cm^{-1} at ±325 μm deflection. The Talbot effect is the repeated imaging of the diffraction grating itself at regular distances. The Talbot length, T, can be expressed as

$$T = \frac{2\Lambda^2}{\lambda}, \tag{1}$$

where λ is the wavelength and Λ the grating period [16]. In our case $\Lambda = 130$ μm and λ_{max} in the chosen interval is 16 μm (625 cm^{-1}). The phase-reversed Talbot image appears at $T/2$, leading to a practical upper deflection limit of 1.06 mm, which is high compared to the maximum deflection of 325 μm. Diffraction order mixing, on the other hand, is an area where some compromise is needed. The detector window plane is sketched in the upper row of Fig. 2 for the two extremities of the wave band, assuming point light sources. The blue box represents the detector width. Separation between order centers at the detector is under the paraxial approximation determined by Eq. (2), where f_{foc} is the focal length of the focusing lens:

$$S_0 = f_{foc}\frac{\lambda}{\Lambda}. \tag{2}$$

The degree of collimation is defined by the half divergence angle and given in Eq. (3):

$$\theta_d = \frac{D}{2f_{foc}}, \tag{3}$$

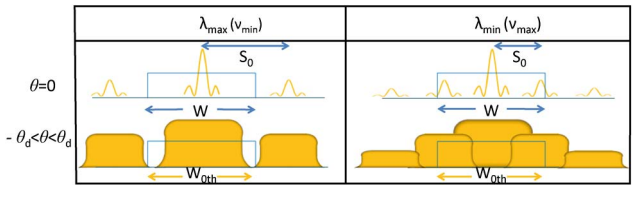

Fig. 2. Sketch of the order mixing for long and short wavelengths. The upper part of the figure shows the ideal case of point source illumination. The lower part of the figure illustrates the actual situation with nonzero divergence.

where D is the diameter of the IR source and f_{col} is the focal length of the collimating lens. The detector window plane is sketched in the bottom row of Fig. 2 by taking the divergence angle of both λ_{min} and λ_{max} into account. The width of the zeroth order in this case can be calculated as in Eq. (4):

$$W_{0th} = 2\theta_d \times f_{foc} = D\frac{f_{foc}}{f_{col}}. \tag{4}$$

It is unavoidable to have some mixing of the zeroth and the first orders for short wavelengths. This reduces the signal-to-bias ratio (SBR), defined as the ratio of the AC signal to DC bias of the interferogram. The width of the zeroth order is optimized by properly selecting focal lengths of the focusing lens and the collimating lens.

In order to optimize the optical design of the spectrometer the algorithm given in [12] is implemented in MATLAB, as illustrated in Fig. 3(a). Eventually the interferogram signal for a wavelength λ and a deflection d can be written as

$$I(\lambda, d) = \int_{x=-W/2}^{W/2} \sum_{\theta=-\theta_d}^{\theta_d} |\mathcal{F}\{E(r_1) + E(t_1, r_2, t_2)\}|^2, \tag{5}$$

where E corresponds to the electric field and F denotes the Fourier transform. The calculation steps are as follows: a plane wave is created and propagated through the double grating. After reflection from the grating the wavefront is split into a first part due to reflection from the upper mirrors (r_1) and a second part that is reflected from the bottom mirrors. The second component is calculated by considering Fresnel propagation due to optical path (d), transmission coefficients (t_1, t_2), and the reflection coefficient (r_2). The wave is then focused onto the detector with the focusing lens. The interferogram

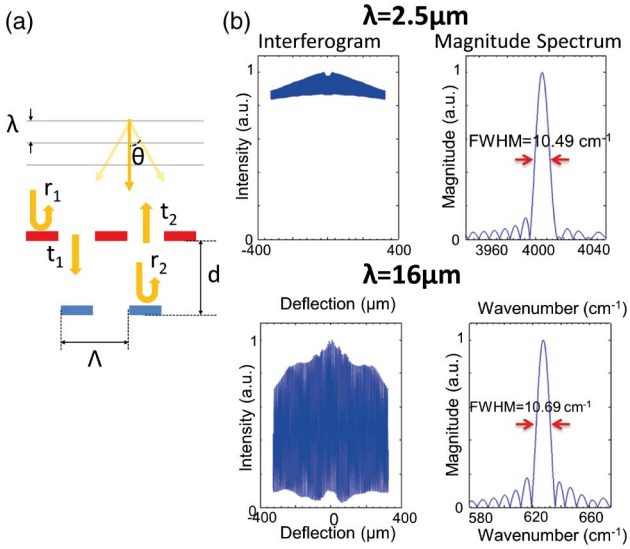

Fig. 3. (a) Illustration of the algorithm used to model performance of the LGI device [12]. (b) Results at the two extremities of the predefined wavelength interval.

intensity for a specific deflection is calculated by integration of the beam energy within the detector window. The whole interferogram can be calculated by sweeping the deflection parameter (d) over the entire range. Finally, the spectrum is calculated by taking the Fourier transform of the interferogram. The two most important parameters are full width at half-maximum (FWHM) of the magnitude spectrum and the SBR.

For a given detector width W, W_{0th} can be adjusted by the choice of lenses. Optimal signal-to-noise ratio (SNR) and SBR are obtained when W_{0th} is about the same size as W. In the actual setup the detector width is 1.4 mm. Smaller W_{0th} results in larger bias and smaller signal due to order mixing. Larger W_{0th} improves SBR. SNR decreases as signal level becomes very small.

As shown in Fig. 3 the system performance is tested for the two extremes of the detector's spectral band (625–4000 cm^{-1}) to investigate the impact of order mixing effects and the Talbot effect. The chosen value for the collimation lens is $f_{col} = 5.8$ mm, which clears the lower limit to fit W_{0th} inside the detector area, while still giving an even spectral resolution over the wavelength interval. The simulated interferograms and spectrums calculated from these are shown in Fig. 3(b). The resolution is equal for the two extreme cases, but the SBR is lower for $\lambda = 2.5$ μm due to order mixing, which decreases dynamic range. In the actual system a capacitor is added to the IR detector output to filter out DC components and maintain AC coupled detection.

3. Spectrum Measurements

To investigate the effects of interferometer deflection on the system, the spectrum of a polystyrene sample is measured with varying deflection (Fig. 4). Each spectrum is obtained by averaging over 32 measurements. Resolution is increasing with increasing deflection as expected. In the range of 4000–3500 cm^{-1} noise also increases. Dynamic deformation of the MEMS mirrors is one of the reasons for

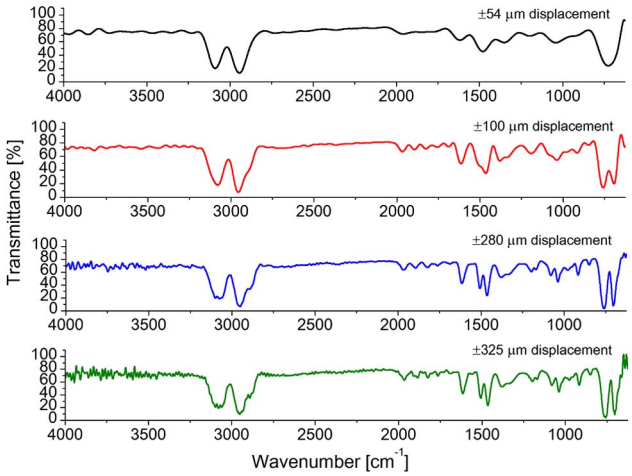

Fig. 4. Polystyrene spectrum measured at varying OPD, each averaged over 32 measurements.

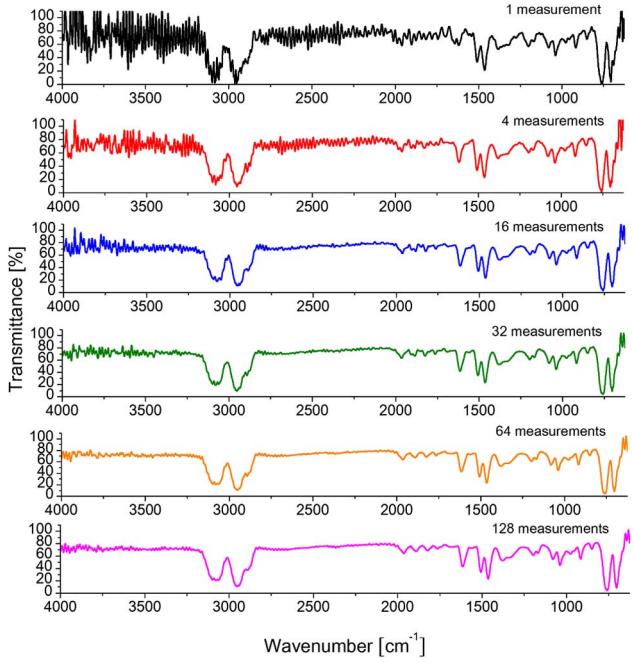

Fig. 5. Spectrums of the same polystyrene sample, measured at a device deflection of ±325 μm. The data was averaged over a varying number of measurements to show the effect of averaging.

this noise. This region also suffers from order mixing, as explained in the previous section, and is hence more sensitive to any disturbance. At short wavenumbers the resolution is increasing gradually, while noise is not increasing significantly.

SNR of the measured spectrum can be improved by averaging multiple scans at the expense of the measurement time. Polystyrene spectrums, obtained by averaging over a varying number of measurements are shown in Fig. 5. Averaging decreases the noise level, especially at high (4000–3500 cm^{-1}) and

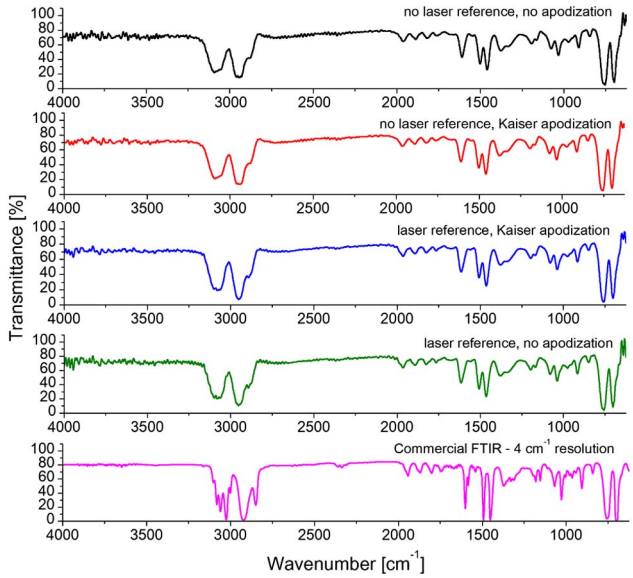

Fig. 6. Comparison of the generated spectrum with that of a commercial device.

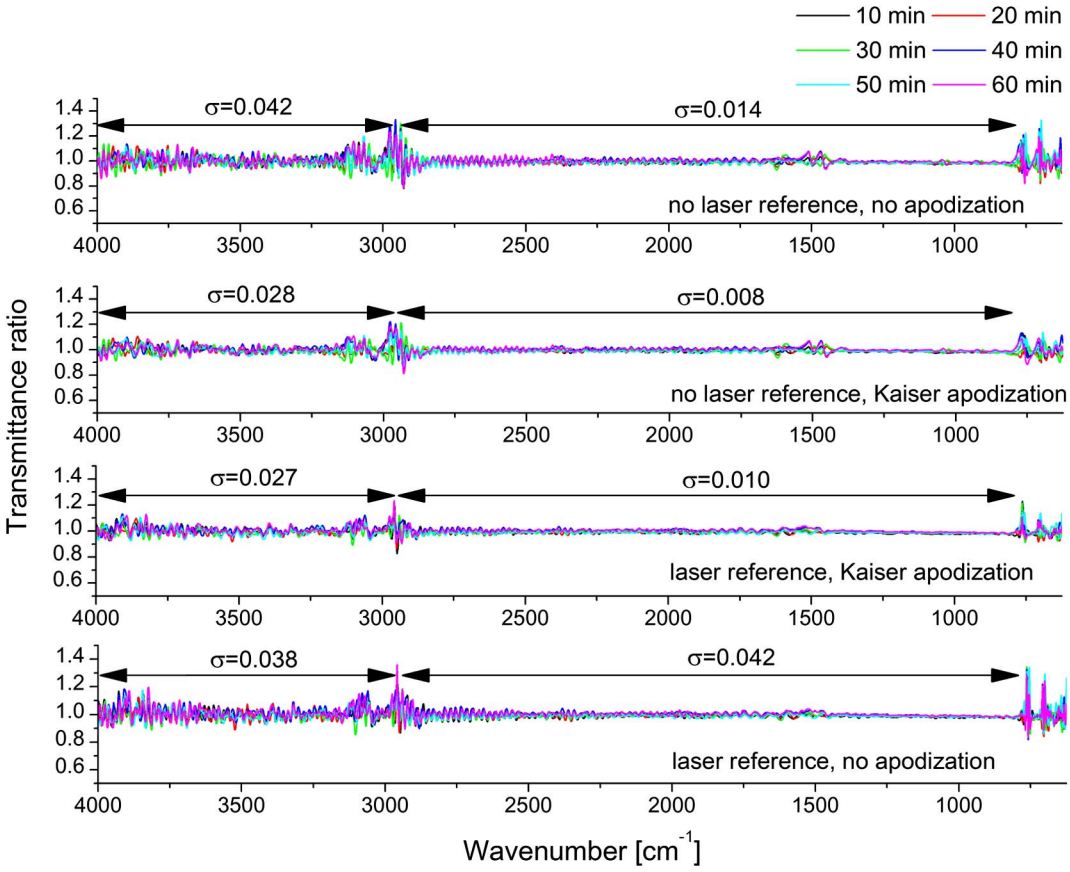

Fig. 7. Stability plot of MEMS FTIR while actuated with air pressure at a deflection of ±325 μm. The resulting data is the average of 64 measurements for each spectrum. The spectrums are calculated at each 10 min interval and divided by a reference spectrum taken at the zeroth minute to obtain the relative change.

moderate wavenumbers (2800–2000 cm^{-1}). An increasing measurement number improves the spectrum quality up to 64 measurements. Increasing that number to 128 did not improve the results further. On the other hand, even without any averaging (one measurement only) most of the characteristic peaks of polystyrene spectrum are observed. Depending on speed and accuracy requirements a measurement takes 1.5 ms (650 spectrums/s) to 100 ms (10 spectrum/s).

A virtual reference interferogram can be generated and used instead of the laser reference if the mirror motion is assumed to be sinusoidal and if the OPD is known and stable. In Fig. 6 the polystyrene spectrum measured with a commercial FTIR spectrometer is compared to spectrums obtained with or without laser reference and with or without apodization. Although peaks around 3000 cm^{-1} are not observed with the virtual reference, the resolution is identical for the two references over most of the range. The laser reference is traditionally used in MEMS spectrometers [17] because of two major advantages: it will keep up with long-term deflection drift (not accounted for here) and it can take into account the small deflection variations between vibration cycles. The latter is what leads to a slightly better resolution at high wavenumbers in this measurement. However, elimination of the He–Ne laser and photodetector enables further miniaturization of the system, which is of large interest for some industrial monitoring applications.

In order to determine the stability of the device a series of measurements were carried out with the device continuously running for 1 h at ±325 μm (Fig. 7). First a typical spectrum measurement is made at the zeroth minute, then a measurement with the sample in place is done every 10 min by averaging over 64 measurements. Each spectrum is then calculated using the background measured at the zeroth minute. Finally, every spectrum is divided by the full zeroth minute spectrum to obtain the relative change. It is observed that stability is improved when apodization is applied to the data. It is also seen that instability, rather than drift dominated the measurement noise.

4. Conclusion

A complete, miniaturized IR spectrometer with a MEMS-based dynamic lamellar grating as the active component was developed. The LGI approach lends itself to the implementation of an achromatic, robust, compact, and easy-to-handle FTIR system. The bulk of the system consists of an IR source and a detector. The spectral resolution is 15 cm^{-1} in the range of 650–2800 cm^{-1}, which is consistent with the

theoretical limit. The stability is better than 1% in this range. As explained above the obtained spectrum resolution is about 20 cm^{-1} in the range of 2800–4000 cm^{-1}. The stability is better than 3% in this range. Lower resolution and higher noise is a result of the current grating pitch of 130 μm, which provides a good balance between long Talbot distance and diffraction order mixing.

The system is fast and as long as the device deflection is known, which can be achieved with infrequent calibrations, no laser reference is needed, enabling the system to be simple and compact. The system is achromatic and can be made portable. High-speed measurements lead to application flexibility with up to 600 measurements per second.

The authors would like to thank all MEMFIS project partners. This work was supported by the MEMFIS Project, funded by the European Commission Seventh Framework Program under grant 224151. The authors would also like to thank H. R. Seren for the mechanical device design, the Center of Micronanotechnology (CMI) at École Polytechnique Fédérale de Lausanne (EPFL) for help with the microfabrication, and P. Flückiger and Y. Leblebici from EPFL for support and help.

References

1. J. Bates, "Fourier transform infrared spectroscopy," Science **191**, 31–37 (1976).
2. R. J. Bell, *Introductory Fourier Transform Spectroscopy* (Academic, 1972).
3. G. Horlick, "Introduction to Fourier transform spectroscopy," Appl. Spectrosc. **22**, 617–626 (1968).
4. D. Bell, T. Lu, N. Fleck, and S. Spearing, "MEMS actuators and sensors: observations on their performance and selection for purpose," J. Micromech. Microeng. **15**, S153–S164 (2005).
5. H. Fujita, "Microactuators and micromachines," Proc. IEEE **86**, 1721–1732 (1998).
6. E. Thielicke and E. Obermeier, "Microactuators and their technologies," Mechatronics **10**, 431–455 (2000).
7. A. A. Michelson, "The relative motion of the Earth and the luminiferous ether," Am. J. Sci. **22**, 120–129 (1881).
8. A. Kenda, S. Lüttjohann, T. Sandner, M. Kraft, A. Tortschanoff, and A. Simon, "A compact and portable IR analyzer: progress of a MOEMS FT-IR system for mid-IR sensing," Proc. SPIE **8032**, 80320O (2011).
9. M. Kraft, A. Kenda, T. Sandner, and H. Schenk, "MEMS-based compact FT-spectrometers—a platform for spectroscopic mid-infrared sensors," in *2008 IEEE Sensors* (IEEE, 2008), pp. 130–133.
10. J. Strong and G. A. Vanasse, "Lamellar grating far-infrared interferomer," J. Opt. Soc. Am. **50**, 113 (1960).
11. C. Ataman and H. Urey, "Modeling and characterization of comb-actuated resonant microscanners," J. Micromech. Microeng. **16**, 9–16 (2006).
12. O. Ferhanoglu, H. R. Seren, S. Lüttjohann, and H. Urey, "Lamellar grating optimization for miniaturized fourier transform spectrometers," Opt. Express **17**, 21289–21301 (2009).
13. O. Manzardo, R. Michaely, F. Schädelin, W. Noell, T. Overstolz, N. De Rooij, and H. P. Herzig, "Miniature lamellar grating interferometer based on silicon technology," Opt. Lett. **29**, 1437–1439 (2004).
14. H. R. Seren, S. Holmstrom, N. P. Ayerden, J. Sharma, and H. Urey, "Lamellar-grating-based MEMS Fourier transform spectrometer," J. Microelectromech. Syst. **21**, 331–339 (2012).
15. E. R. Deutsch, D. Reyes, E. R. Schildkraut, and J. Kim, "High-resolution miniature FTIR spectrometer enabled by a large linear travel MEMS pop-up mirror," Proc. SPIE **7319**, 73190J (2009).
16. L. Rayleigh, "XXV. On copying diffraction-gratings, and on some phenomena connected therewith," Philos. Mag. **11**(67), 196–205 (1881).
17. J. Connes and P. Connes, "Near-infrared planetary spectra by Fourier spectroscopy. I. Instruments and results," J. Opt. Soc. Am. **56**, 896–910 (1966).